


 Cite this: *RSC Adv.*, 2022, 12, 602

# Highly efficient selective hydrogenation of levulinic acid to $\gamma$ -valerolactone over Cu–Re/TiO<sub>2</sub> bimetallic catalysts†

 Yingxin Liu,<sup>ab</sup> Kai Liu,<sup>a</sup> Meihua Zhang,<sup>a</sup> Kaiyue Zhang,<sup>a</sup> Jiao Ma,<sup>a</sup> Shuwen Xiao,<sup>cd</sup> Zuojun Wei<sup>\*cd</sup> and Shuguang Deng<sup>ab</sup>

Highly active and thermally stable Cu–Re bimetallic catalysts supported on TiO<sub>2</sub> with 2.0 wt% loading of Cu were prepared *via* an incipient wetness impregnation method and were applied for liquid phase selective hydrogenation of levulinic acid (LA) to  $\gamma$ -valerolactone (GVL) in H<sub>2</sub>. The effect of the molar ratios of Cu : Re on the physico-chemical properties and the catalytic performance of the Cu–Re/TiO<sub>2</sub> catalysts was investigated. Moreover, the influence of various reaction parameters on the hydrogenation of LA to GVL was studied. The results showed that the Cu–Re/TiO<sub>2</sub> catalyst with a 1 : 1 molar ratio of Cu to Re (Cu–Re(1 : 1)/TiO<sub>2</sub>) exhibited the highest performance for the reaction. Complete conversion of LA with a 100% yield of GVL was achieved in 1,4-dioxane solvent under the reaction conditions of 180 °C, 4.0 MPa H<sub>2</sub> for 4 h, and the catalyst could be reused at least 6 times with only a slight loss of activity. Combined with the characterization results, the high performance of the catalyst was mainly attributed to the well-dispersed Cu–Re nanoparticles with a very fine average size (*ca.* 0.69 nm) and the co-presence of Cu–Re bimetal and ReO<sub>x</sub> on the catalyst surface.

 Received 30th July 2021  
 Accepted 14th December 2021

DOI: 10.1039/d1ra05804e

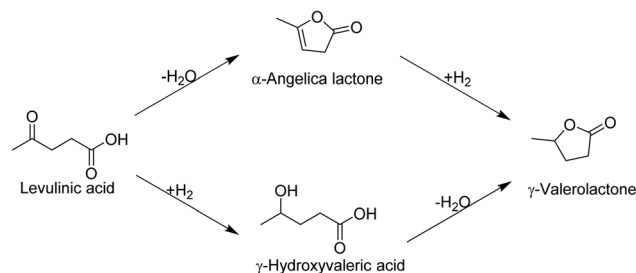
[rsc.li/rsc-advances](http://rsc.li/rsc-advances)

## 1. Introduction

Increasing global energy demands and diminishing fossil fuel stores have provided the scientific community with an unprecedented power in developing new economically viable routes to sustainable energy.<sup>1,2</sup> Biomass, as a clean, renewable and new carbon source with the advantages of abundant reserves, low price and short generation period, is considered to be an indispensable energy source for human development in the future. Biomass can be converted into biofuels and high value-added chemicals through different technologies.<sup>2,3</sup>  $\gamma$ -Valerolactone (GVL) is one of the most important sustainable biomass-derived chemicals, which can be used to participate in various reactions, as well as being applied as a food flavor, lubricant, plasticizer and reaction solvent, owing to its excellent physical and chemical properties.<sup>4–7</sup>

Typically, GVL can be obtained through hydrogenation and cyclization of biomass derivative levulinic acid (LA) over homogeneous or heterogeneous catalysts as shown in Scheme 1.<sup>8–10</sup> In consideration of easy product separation and catalyst recycling, heterogeneous catalysts are preferred. Supported Ru, Rh, Pd, Pt, Au and Ir noble metal catalysts have been employed for the hydrogenation of LA into GVL.<sup>11–16</sup> Among them, Ru-based catalysts have been proved to be one of the most active heterogeneous catalysts.<sup>17–21</sup> Our previous work also showed that the Ru catalyst embedded in N-doped mesoporous carbon exhibited high performance for the hydrogenation of LA into GVL.<sup>22</sup>

At the same time, some researchers have focused on non-noble metal catalysts.<sup>23</sup> The Cu-based non-noble metal catalysts, which are generally considered to be active for the



Scheme 1 Reaction pathways for the hydrogenation of LA to GVL.

<sup>a</sup>College of Pharmaceutical Science, Zhejiang University of Technology, Hangzhou 310014, P. R. China. E-mail: weizuojun@zju.edu.cn; Shuguang.Deng@asu.edu

<sup>b</sup>School for Engineering of Matter, Transport and Energy, Arizona State University, 551 E. Tyler Mall, Tempe, AZ 85287, USA

<sup>c</sup>Key Laboratory of Biomass Chemical Engineering of the Ministry of Education, College of Chemical and Biological Engineering, Zhejiang University, Hangzhou 310027, P. R. China

<sup>d</sup>Institute of Zhejiang University-Quzhou, 78 Jinhua Boulevard North, Quzhou 324000, P. R. China

† Electronic supplementary information (ESI) available. See DOI: 10.1039/d1ra05804e



selective hydrogenation of C=O bonds and relatively inactive for the hydrogenolysis of C–C bonds,<sup>24,25</sup> have been reported to be effective for the hydrogenation of LA to GVL. For example, Hutchings *et al.*<sup>26</sup> investigated the performance of Cu–ZrO<sub>2</sub> catalyst for the hydrogenation of LA to GVL, and obtained over 90% of LA conversion after reaction 60 min at 200 °C and 35 bar H<sub>2</sub>. Xu *et al.*<sup>27</sup> studied LA hydrogenation over Cu(30%)/WO<sub>3</sub>(10%)/ZrO<sub>2</sub>-CP-300 catalyst in ethanol and obtained the maximum GVL yield of 94% at 200 °C and 5 MPa H<sub>2</sub> for 6 h. However, most of the copper monometallic catalysts exposed a lot of problems, such as a high copper loading and harsh reaction conditions.

Recently, bimetallic catalysts have caused widespread concern due to their unique catalytic performance. It is widely believed that the addition of another metal will enhance the catalytic activity and stability of the catalyst by changing the electronic and geometric properties of the first metal.<sup>28,29</sup> Zhang *et al.*<sup>30</sup> reported that using CuAg/Al<sub>2</sub>O<sub>3</sub> as catalyst and THF as a solvent, LA conversion could reach 100%, and GVL selectivity was up to 99% at 180 °C and 1.4 MPa H<sub>2</sub> for 4 h. Cai *et al.*<sup>31</sup> developed 10Cu–5Ni/Al<sub>2</sub>O<sub>3</sub> bimetallic catalyst for the transfer hydrogenation of ethyl levulinate to GVL with 2-butanol as the hydrogen donor, and obtained a 97% yield of GVL in 12 h at 150 °C. Yanase *et al.*<sup>32</sup> tested bimetallic Cu–Co/Al<sub>2</sub>O<sub>3</sub> catalyst for gas-phase hydrogenation of LA to GVL and obtained a GVL productivity of 5.46 kg<sub>GVL</sub> kg<sub>catalyst</sub><sup>−1</sup> h<sup>−1</sup> with a GVL selectivity higher than 99% at 250 °C for 24 h.

In this study, we report the Cu–Re/TiO<sub>2</sub> bimetallic catalyst for the liquid phase hydrogenation of LA to GVL. The choice of metal Re as the second component is mainly based on the following considerations. Firstly, ReO<sub>x</sub> as well as TiO<sub>2</sub> has many oxygen vacancies, which facilitates the adsorption of oxygen-containing functional groups, such as –OH and C=O,<sup>33,34</sup> facilitating the catalytic conversion of LA. Secondly, Re oxophilic metal oxide can be partially reduced to a metallic state in a reducing atmosphere, and Re<sup>0</sup> can serve as a second metal component to form a bimetal or alloy with another hydrogenation-active metal and provide a synergistic effect, which is beneficial to improve the hydrogenation catalytic performance and stability of the catalyst.<sup>35–37</sup> Our previous work showed that the bimetallic catalyst Pt–Re exhibited high performance for hydrogenation of cinnamaldehyde to cinnamyl alcohol.<sup>38</sup> And our recent study showed that bimetallic catalyst Fe–Re/TiO<sub>2</sub> exhibited superior catalytic performance for LA hydrogenation to GVL compared to monometallic Fe and Re catalysts at similar metal content. Under optimized conditions, nearly full conversion of LA with a 95% yield of GVL could be achieved at 180 °C in water at a H<sub>2</sub> pressure of 40 bar.<sup>39</sup>

Here, Cu–Re bimetallic catalysts supported on TiO<sub>2</sub> with different Cu/Re molar ratios were prepared *via* an incipient wetness impregnation method. A structure–activity relationship was extensively discussed based on various characterization results and activity testing results. Moreover, the effect of reaction parameters on LA conversion was investigated.

## 2. Experimental

### 2.1. Materials

Levulinic acid (99.0%) was purchased from Shanghai Jingchun Reagent Co., Ltd. Cu(NO<sub>3</sub>)<sub>2</sub>·3H<sub>2</sub>O (99.99%) was purchased from Shanghai Aibi Chemical Reagent Co., Ltd, China. NH<sub>4</sub>ReO<sub>4</sub> (99.99%) was purchased from Shanghai Macklin Biochemical Co., Ltd. 1,4-Dioxane (99.0%), methanol (99.9%) and TiO<sub>2</sub> (99.0%) were purchased from Shanghai Aladdin Reagent Co., Ltd. All the chemicals used in this work were analytical reagents and were used without further purification.

### 2.2. Catalyst preparation

A series of Cu–Re/TiO<sub>2</sub> bimetallic catalysts with different Cu : Re molar ratios were prepared by an incipient wetness impregnation method. In a typical procedure, an aqueous solution containing the required amount of Cu(NO<sub>3</sub>)<sub>2</sub>·3H<sub>2</sub>O and NH<sub>4</sub>ReO<sub>4</sub> was added to the support TiO<sub>2</sub> in a beaker. After impregnated for 24 h, the mixture was dried at 110 °C for 10 h and finally reduced at 500 °C in a tubular furnace under hydrogen flow for 3 h to obtain the target catalyst, which was denoted as Cu–Re(*x* : *y*)/TiO<sub>2</sub>, where *x* : *y* means the molar ratio of Cu to Re. The molar ratio of Cu to Re was varied from (3 : 1) to (1 : 1) by changing the Re content and using a fixed amount of Cu (2.0 wt%), in order to investigate the influence of Re content on the property of the Cu–Re/TiO<sub>2</sub>. Two monometallic catalysts 2.0 wt% Cu/TiO<sub>2</sub> and 5.8 wt% Re/TiO<sub>2</sub> were prepared by using the same method for comparison.

### 2.3. Catalyst characterization

The specific surface area was determined by N<sub>2</sub> adsorption at –196 °C with the Brunauer–Emmett–Teller (BET) method using an ASAP 2010 instrument (Micromeritics Instrument Co.). The pore size distribution and pore volume were measured at –196 °C by using Barrett–Joyner–Halenda (BJH) analysis from the desorption branch of the N<sub>2</sub> adsorption–desorption isotherms. Prior to N<sub>2</sub> physisorption, the samples were degassed under vacuum at 250 °C for 10 h.

Transmission electron microscopy (TEM) images were obtained using a Tecnai G2 F30 S-Twin instrument (Philips-FEI Co., The Netherlands). Samples were prepared by dispersing the reduced catalyst powder in ethanol under ultrasound for 15–20 min and then dropping the suspension onto a copper grid coated with carbon film. The particle size distribution of the metal nanoparticles in each sample was determined from the corresponding TEM image by measuring the sizes of more than 100 particles.

H<sub>2</sub> temperature-programmed reduction (H<sub>2</sub>-TPR) of the samples was performed on a Chemisorb FINESORB-3010 instrument. The dried catalyst samples were reduced at 10 °C min<sup>−1</sup> under a gaseous mixture of 10 vol% hydrogen in nitrogen (gas flow rate: 60 mL min<sup>−1</sup>). Hydrogen consumption was monitored on a thermal conductivity detector (TCD).

X-ray photoelectron spectroscopy (XPS) spectra were obtained using an Escalab Mark II X-ray spectrometer (VG Co., United Kingdom) equipped with a magnesium anode (Mg Kα =

1253.6 eV). Energy corrections were performed using a 1s peak of the pollutant carbon at 284.6 eV. The sample was prepared by pressing the catalyst powder onto the surface with silver sol-gel.

#### 2.4. Reaction procedure

The hydrogenation of LA to GVL was performed in a 25 mL stainless-steel autoclave equipped with magnetic stirring. In a typical reaction, 0.5 g of LA, 50 mg of catalyst and 10 mL of solvent 1,4-dioxane were introduced into the reactor. Then the reactor was sealed, purged with H<sub>2</sub> five times, and pressurized with H<sub>2</sub> to the required pressure. The autoclave was then heated to the required temperature and kept at this temperature for the required time under the continuous stirring speed of 1000 rpm to eliminate external diffusion. After the reaction, the autoclave was cooled to room temperature, the residual hydrogen gas was released and the reaction mixture was centrifuged. The solid catalyst was washed with 1,4-dioxane for the next cycle, and the separated liquid reaction solution was quantitatively analyzed with an Agilent 7890A gas chromatography equipped with an HP-5 capillary column (30.0 m × 0.32 mm × 0.25 μm) and a flame ionization detector (FID) using *n*-dodecane as an internal standard. The confirmation of the liquid products was performed on an Agilent 6890 GC system coupled to a mass spectrometer equipped with an Agilent 5973 quadrupole mass analyzer. The potential Cu and Re leach was detected by inductively coupled plasma-mass spectroscopy (ICP-MS, PerkinElmer Elan DRC-e).

### 3. Results and discussion

#### 3.1. Catalytic performance of Cu–Re/TiO<sub>2</sub> catalysts

To ascertain the effect of Re on the performance of Cu/TiO<sub>2</sub> catalyst, a series of Cu–Re/TiO<sub>2</sub> catalysts with different Cu : Re molar ratios were prepared and tested for hydrogenation of LA

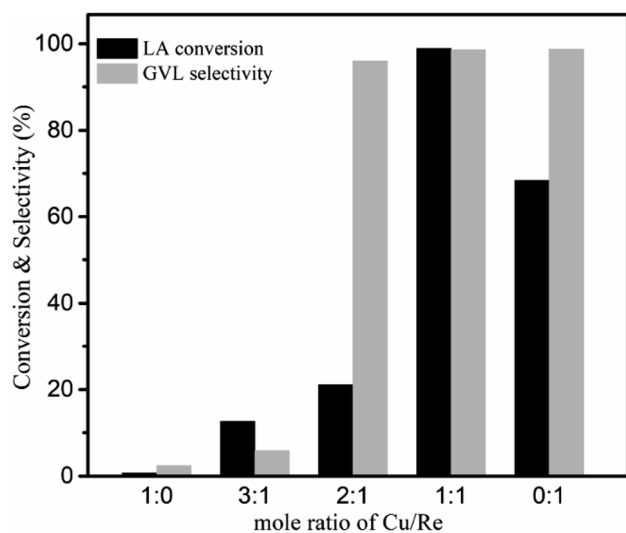


Fig. 1 Hydrogenation of LA to GVL over Cu–Re/TiO<sub>2</sub> catalysts with different Cu : Re molar ratios. Reaction conditions: 0.5 g LA, 50 mg catalyst, 10 mL 1,4-dioxane, 4.0 MPa H<sub>2</sub>, 180 °C, 3 h, and 1000 rpm.

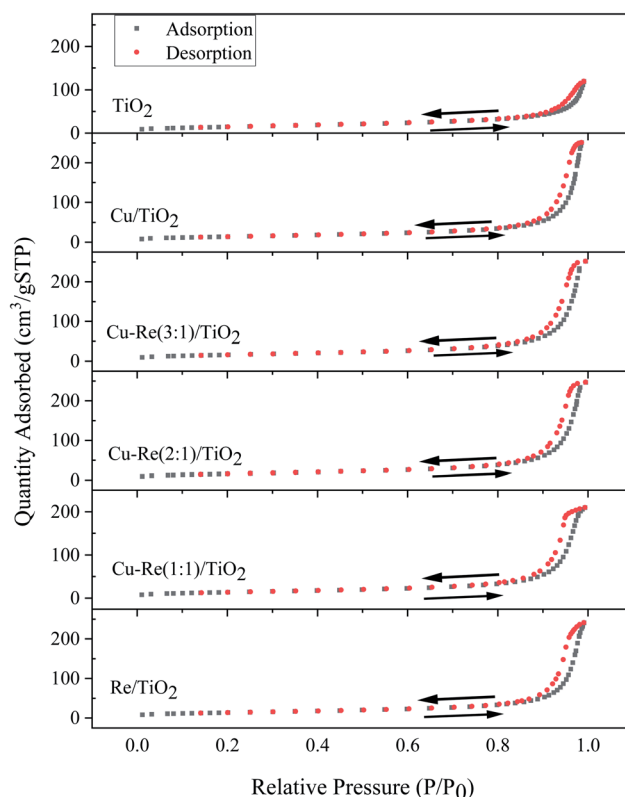


Fig. 2 N<sub>2</sub> adsorption–desorption isotherms of TiO<sub>2</sub>, Cu/TiO<sub>2</sub>, Re/TiO<sub>2</sub> and Cu–Re/TiO<sub>2</sub> catalysts.

into GVL in a batch reactor in 1,4-dioxane solvent at 180 °C and 4.0 MPa H<sub>2</sub> for 3 h, and the results are shown in Fig. 1. Mono-metallic 2 wt% Cu/TiO<sub>2</sub> showed almost no activity for the reaction, over which the conversion of LA and the selectivity to GVL was only 0.7% and 2.4%, respectively. Although mono-metallic 5.8 wt% Re/TiO<sub>2</sub> showed good selectivity toward GVL (98.7%), its activity was low, with a LA conversion of 68.4%. It can be seen that the addition of Re remarkably improved the catalytic performance of the Cu-based catalysts for LA hydrogenation, and the performance of the Cu–Re/TiO<sub>2</sub> bimetallic catalysts increased with the increase in Re : Cu molar ratio. It was noteworthy that the Cu–Re(1 : 1)/TiO<sub>2</sub> catalyst exhibited the

Table 1 Structural properties of TiO<sub>2</sub>, Cu/TiO<sub>2</sub>, Re/TiO<sub>2</sub> and Cu–Re/TiO<sub>2</sub> catalysts

| Catalyst                      | $S_{\text{BET}}^a$ (m <sup>2</sup> g <sup>-1</sup> ) | $V_p^b$ (cm <sup>3</sup> g <sup>-1</sup> ) | $D_p^b$ (nm) |
|-------------------------------|--|--|--------------|
| TiO <sub>2</sub>              | 53   | 0.15                                       | 11.3         |
| Cu/TiO <sub>2</sub>           | 52   | 0.33                                       | 25.2         |
| Cu–Re(3 : 1)/TiO <sub>2</sub> | 60   | 0.39                                       | 26.0         |
| Cu–Re(2 : 1)/TiO <sub>2</sub> | 59   | 0.36                                       | 25.6         |
| Cu–Re(1 : 1)/TiO <sub>2</sub> | 60   | 0.32                                       | 25.6         |
| Re/TiO <sub>2</sub>           | 61   | 0.33                                       | 26.4         |

<sup>a</sup> The specific surface area was calculated by using the BET method.

<sup>b</sup> The pore size and pore volumes were derived from the adsorption branches of isotherms by using the BJH model.

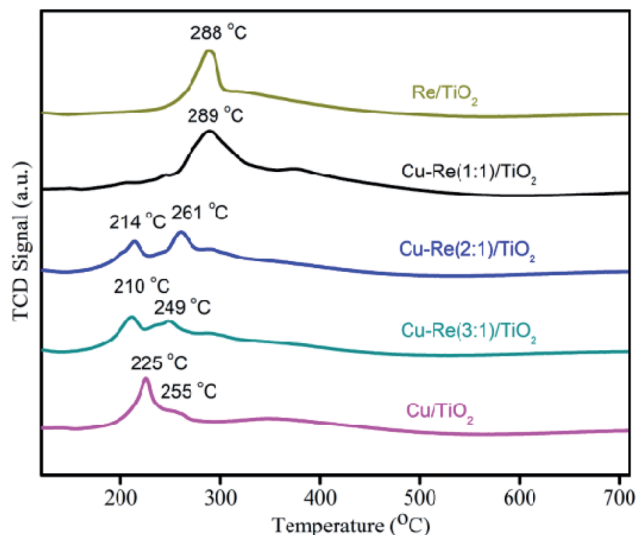


Fig. 3  $\text{H}_2$ -TPR profiles of  $\text{Cu}/\text{TiO}_2$ ,  $\text{Re}/\text{TiO}_2$  and  $\text{Cu-Re}/\text{TiO}_2$  catalysts.

highest activity and selectivity to GVL, giving a GVL yield as high as 97.5% at a LA conversion of 98.9%.

### 3.2. Characterization of $\text{Cu-Re}/\text{TiO}_2$ catalysts

$\text{N}_2$  adsorption/desorption isotherms of support  $\text{TiO}_2$ , monometallic  $\text{Cu}/\text{TiO}_2$  and  $\text{Re}/\text{TiO}_2$ , and  $\text{Cu-Re}/\text{TiO}_2$  bimetallic

catalysts are presented in Fig. 2, and the relative texture parameters (specific surface areas ( $S_{\text{BET}}$ ), pore volume and average pore diameter) of these samples are listed in Table 1. All the samples shown in Fig. 2 exhibited type IV isotherms, a typical characteristic for mesoporous materials.<sup>40</sup> The  $S_{\text{BET}}$  of  $\text{TiO}_2$  was kept no obvious change after supporting metal elements, while the pore volume and average pore diameter increased significantly, indicating a strong influence of the metal ions on  $\text{TiO}_2$  textural properties.<sup>41</sup>

Fig. 3 shows the  $\text{H}_2$ -TPR profiles of monometallic  $\text{Cu}/\text{TiO}_2$  and  $\text{Re}/\text{TiO}_2$ , and bimetallic  $\text{Cu-Re}/\text{TiO}_2$  catalysts dried at  $110^\circ\text{C}$ . In monometallic  $\text{Cu}/\text{TiO}_2$ , two peaks occurred at  $225^\circ\text{C}$  and  $255^\circ\text{C}$ , which were likely attributed to the reduction of highly dispersed  $\text{CuO}$  species in intimate contact with  $\text{TiO}_2$  and the reduction of the oxide clusters with a structure similar to  $\text{CuO}$ , respectively.<sup>42</sup> In the case of monometallic  $\text{Re}/\text{TiO}_2$ ,  $\text{Re}$  species reduced between  $220$  and  $350^\circ\text{C}$  with a peak maximum at  $288^\circ\text{C}$ , in agreement with the literature.<sup>43</sup> On bimetallic  $\text{Cu-Re}(3:1)/\text{TiO}_2$  and  $\text{Cu-Re}(2:1)/\text{TiO}_2$  catalysts, two peaks were observed between  $210$  and  $261^\circ\text{C}$ , and the peaks moved towards low temperature compared with the two monometallic catalysts  $\text{Cu}/\text{TiO}_2$  and  $\text{Re}/\text{TiO}_2$ , which indicates that the addition of  $\text{Re}$  into  $\text{Cu}/\text{TiO}_2$  catalyst is of benefit to the reduction of metal oxide species. It is interesting to note that  $\text{Cu-Re}(1:1)/\text{TiO}_2$  bimetallic catalyst displayed a main broad peak at  $289^\circ\text{C}$  and two additional ones with low intensity. The main peak shifted to

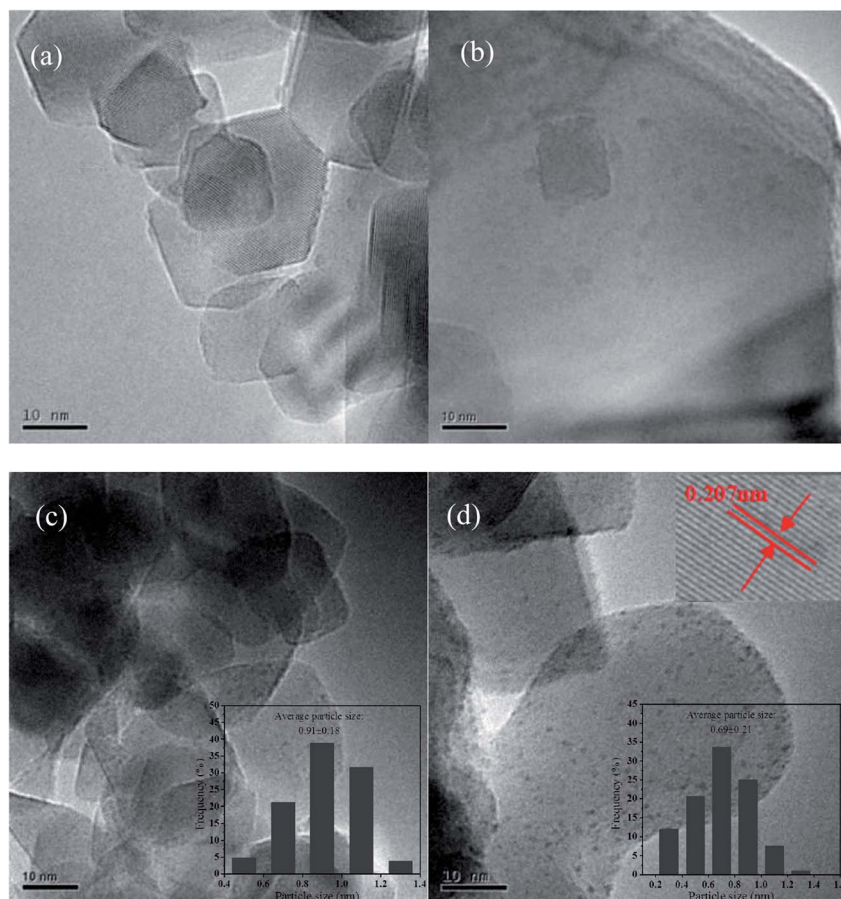


Fig. 4 TEM images of (a)  $\text{Cu}/\text{TiO}_2$ , (b)  $\text{Cu-Re}(3:1)/\text{TiO}_2$ , (c)  $\text{Cu-Re}(2:1)/\text{TiO}_2$  and (d)  $\text{Cu-Re}(1:1)/\text{TiO}_2$  catalysts.



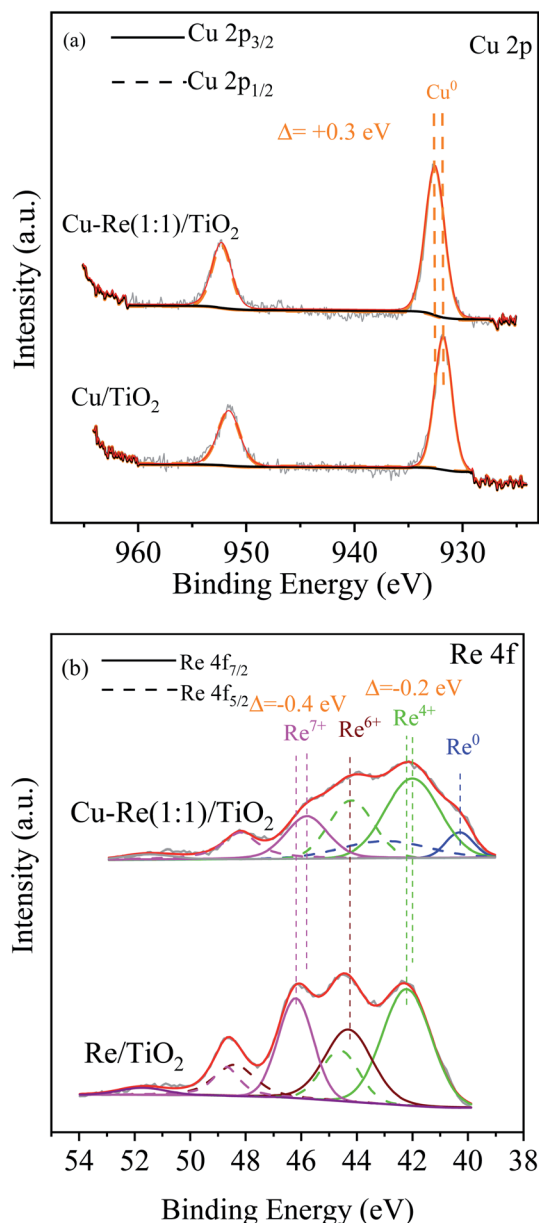


Fig. 5 XPS spectra of Cu/TiO<sub>2</sub>, Re/TiO<sub>2</sub> and Cu–Re(1 : 1)/TiO<sub>2</sub> catalysts.

higher temperature compared with monometallic catalyst Cu/TiO<sub>2</sub>, likely corresponding to monometallic Re-containing sample, indicating that there was a strong interaction between Cu and Re on this sample and that most of Re atoms

were distributed in the periphery of unreduced Cu atoms throughout the catalyst.<sup>44</sup> Furthermore, the reduction bands of Cu–Re(1 : 1)/TiO<sub>2</sub> catalyst were changed to the symmetrical shape compared to those of other samples, which can be induced by a uniform reduction process caused by the homogeneity of metal particle size.<sup>44</sup> Combined with the activity testing results of the catalysts as mentioned above, the improvement in the catalytic activity of the Cu–Re(1 : 1)/TiO<sub>2</sub> catalyst was probably attributed to the strong interaction between Cu and Re.

Fig. 4 displays the TEM images of the reduced Cu/TiO<sub>2</sub> and Cu–Re/TiO<sub>2</sub> catalysts. In the TEM image of monometallic Cu/TiO<sub>2</sub> catalyst (Fig. 4(a)), only a few severely agglomerated Cu nanoparticles with a large average size (about 1.6 nm) were observed, which reduced the activity and selectivity of the catalyst significantly. For the three Cu–Re/TiO<sub>2</sub> bimetallic catalysts (Fig. 4(b)–(d)), metal particles were smaller, with more narrow particle size distributions than Cu/TiO<sub>2</sub>, indicating that metal particles on Cu–Re bimetallic catalysts were uniformly distributed. In particular, Cu–Re(1 : 1)/TiO<sub>2</sub> catalyst showed the largest metal dispersion and the smallest average metal particle size (0.69 nm). As shown in Fig. 4(d), the fringe spacing of Cu–Re(1 : 1) (0.207 nm) is between those of Cu(110) (0.200 nm) and Re(101) (0.211 nm),<sup>45,46</sup> indicating that a Cu–Re alloy was formed in the reduced Cu–Re(1 : 1)/TiO<sub>2</sub> catalyst and this was responsible for strong interaction between metallic Cu and Re species. The result is in good agreement with the TPR results.

Fig. 5 shows the XPS spectra for Cu 2p (Fig. 5(a)) and Re 4f (Fig. 5(b)) levels of the reduced Cu/TiO<sub>2</sub>, Re/TiO<sub>2</sub> and Cu–Re(1 : 1)/TiO<sub>2</sub> catalysts, and the corresponding binding energies are listed in Table 2. The XPS data for Cu 2p on both Cu/TiO<sub>2</sub> and Cu–Re(1 : 1)/TiO<sub>2</sub> catalysts reveal that the Cu species is essentially metallic Cu<sup>0</sup>.<sup>47</sup> XPS analysis for Re 4f displays that Re is present in Re<sup>4+</sup>, Re<sup>6+</sup> and Re<sup>7+</sup> states in the case of monometallic Re/TiO<sub>2</sub>,<sup>48</sup> and in Re<sup>0</sup>, Re<sup>4+</sup> and Re<sup>7+</sup> states in the case of bimetallic Cu–Re(1 : 1)/TiO<sub>2</sub>,<sup>44</sup> indicating that the reduction of Re species is not complete, in agreement with the literature.<sup>43,44</sup> Compared to the corresponding monometallic catalysts, the binding energy for the Cu 2p<sub>3/2</sub> descends to higher values by *ca.* 0.3 eV, while the binding energy of ReO<sub>2</sub> for Re 4f<sub>7/2</sub> shifts to lower values by *ca.* 0.2 eV, indicating a strong interaction may exist between Cu and Re species,<sup>49</sup> per the TPR and TEM results.

### 3.3. Effects of various reaction conditions on hydrogenation of LA

The effect of the reaction temperature in the range of 140–200 °C on the conversion of LA and the selectivity to GVL over

Table 2 XPS results of Cu/TiO<sub>2</sub>, Re/TiO<sub>2</sub> and Cu–Re(1 : 1)/TiO<sub>2</sub> catalysts

| Catalyst                      | Cu 2p <sub>3/2</sub> (2p <sub>1/2</sub> ) (BE/eV) |  | Re 4f <sub>7/2</sub> (4f <sub>5/2</sub> ) (BE/eV) |                  |                  |                                |
|-------------------------------|---|--|---|------------------|------------------|--------------------------------|
|                               | Cu <sup>0</sup>                                   |  | Re <sup>0</sup>                                   | ReO <sub>2</sub> | ReO <sub>3</sub> | Re <sub>2</sub> O <sub>7</sub> |
| Cu/TiO <sub>2</sub>           | 931.7(951.6)                                      |  | —   | —                | —                | —                              |
| Cu–Re(1 : 1)/TiO <sub>2</sub> | 932.0(951.9)                                      |  | 40.3(43.0)  | 42.0(44.2)       | —                | 45.8(48.2)                     |
| Re/TiO <sub>2</sub>           | —   |  | —   | 42.2(44.6)       | 44.3(48.7)       | 46.2(48.4)                     |

Cu-Re(1 : 1)/TiO<sub>2</sub> catalyst was investigated, and the results are shown in Fig. 6. It can be seen that the conversion of LA increased from 22.0% at 140 °C to 53.4% at 160 °C, and the GVL selectivity increased from 78.4% to 89.9%. With the increase in the temperature to 180 °C, GVL selectivity increased to 98.6% with a LA conversion of 98.9%. Further increasing reaction temperature to 200 °C, both LA conversion and GVL selectivity were up to 100%. Considering energy-saving and GVL yield, 180 °C was chosen as the reaction temperature in the following study.

Fig. 7 compares LA hydrogenation results by reaction time over Cu/TiO<sub>2</sub>, Re/TiO<sub>2</sub> and Cu-Re(1 : 1)/TiO<sub>2</sub> catalysts. The bimetallic Cu-Re(1 : 1)/TiO<sub>2</sub> catalyst exhibited the highest performance and produced a GVL yield of 97.5% after 3 h of reaction time. Extending the reaction time to 4 h, a GVL yield of 100% was achieved. In contrast, the monometallic Cu/TiO<sub>2</sub> and Re/TiO<sub>2</sub> catalysts showed a significantly lower activity, achieving a maximum GVL yield of 26.7% and 84.6%, respectively, after 4 h of reaction time. Combined with the characterization results of the catalysts, the excellent performance of Cu-Re(1 : 1)/TiO<sub>2</sub> catalyst for LA hydrogenation to GVL was mainly attributed to the following three aspects. Firstly, Cu-Re miscible phase was formed in the Cu-Re(1 : 1)/TiO<sub>2</sub> catalyst during the reduction process, facilitating the synergistic interaction between copper and rhenium. Secondly, Cu-Re nanoparticles were highly dispersed on the TiO<sub>2</sub> support with uniform and small size (0.69 nm), which increased the active sites on the surface of the catalyst, thereby improving the catalytic activity. Thirdly, the addition of Re was beneficial to the reduction of CuO to Cu<sup>0</sup>, and inhibiting the oxidation of metal Cu<sup>0</sup>. And the presence of ReO<sub>x</sub> species in the catalyst facilitated the adsorption of LA and the transformation of a reaction intermediate 4-hydroxyvaleric acid to GVL.<sup>33</sup>

Table 3 shows the effect of solvent on the performance of Cu-Re(1 : 1)/TiO<sub>2</sub> catalyst for hydrogenation of LA to GVL. When

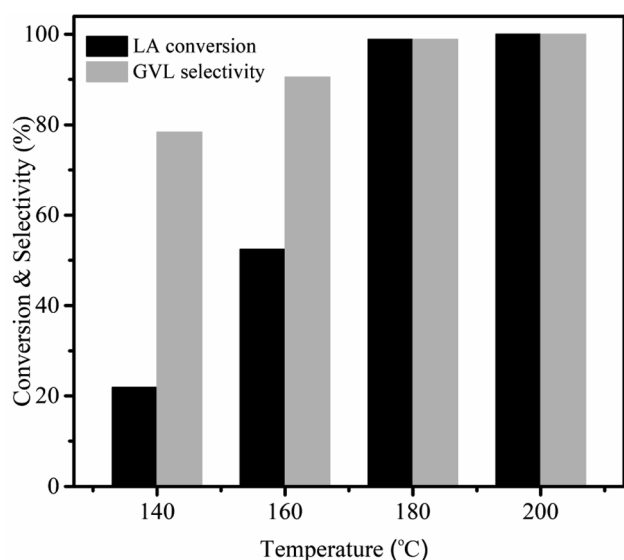


Fig. 6 Effect of reaction temperature on hydrogenation of LA to GVL over Cu-Re(1 : 1)/TiO<sub>2</sub> catalyst. Reaction conditions: 0.5 g LA, 50 mg catalyst, 10 mL 1,4-dioxane, 4.0 MPa H<sub>2</sub>, 3 h, and 1000 rpm.

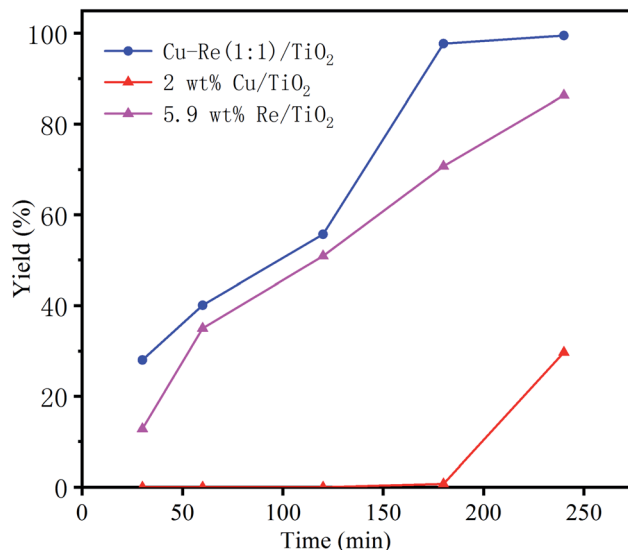


Fig. 7 Production of GVL as a function of reaction time during hydrogenation of LA over Cu/TiO<sub>2</sub>, Re/TiO<sub>2</sub> and Cu-Re(1 : 1)/TiO<sub>2</sub> catalysts. Reaction conditions: 0.5 g LA, 50 mg catalyst, 10 mL 1,4-dioxane, 4.0 MPa H<sub>2</sub>, and 1000 rpm.

methanol was used as a solvent, GVL yield was only 88.1%, and the reaction intermediate 4-hydroxyvaleric acid was the only by-product (11.9%). In the solvent-free conditions, the conversion of LA and the selectivity to GVL reached 97.3% and 97.6%, respectively. A higher yield of GVL (97.5%) was achieved by using 1,4-dioxane as solvent. H<sub>2</sub>O as solvent gave the highest yield of GVL. However, the stability of Cu-Re(1 : 1)/TiO<sub>2</sub> catalyst in H<sub>2</sub>O was poor, and the catalytic activity of the recovered catalyst dropped down substantially, giving a lower yield of GVL (less than 50%) than the first cycle (100%).

#### 3.4. Recyclability of bimetallic Cu-Re(1 : 1)/TiO<sub>2</sub> catalyst

The recyclability of the bimetallic Cu-Re(1 : 1)/TiO<sub>2</sub> catalyst in the hydrogenation of LA into GVL was examined by performing six consecutive catalytic runs. At each cycle, after hydrogenation reaction in 1,4-dioxane solvent at 180 °C and 4.0 MPa H<sub>2</sub> for 3 h, the catalyst was centrifuged, washed with 1,4-dioxane, and reused. As shown in Fig. 8, the Cu-Re(1 : 1)/TiO<sub>2</sub> catalyst exhibited excellent stability. After being recycled six times, Cu-

Table 3 Hydrogenation of LA to GVL in various solvents over Cu-Re(1 : 1)/TiO<sub>2</sub> catalyst<sup>a</sup>

| Solvent          | Conversion (%) | Selectivity (%) |                  |
|------------------|----------------|-----------------|------------------|
|                  |                | GVL             | HVA <sup>b</sup> |
| 1,4-Dioxane      | 98.9           | 98.6            | 1.1              |
| H <sub>2</sub> O | >99.9          | >99.9           | 0                |
| Methanol         | 100            | 88.1            | 11.9             |
| No solvent       | 97.3           | 97.6            | 2.4              |

<sup>a</sup> Reaction conditions: 0.5 g LA, 50 mg catalyst, 10 mL solvent, 4.0 MPa H<sub>2</sub>, 180 °C, 3 h, and 1000 rpm. <sup>b</sup> HVA: 4-hydroxyvaleric acid.

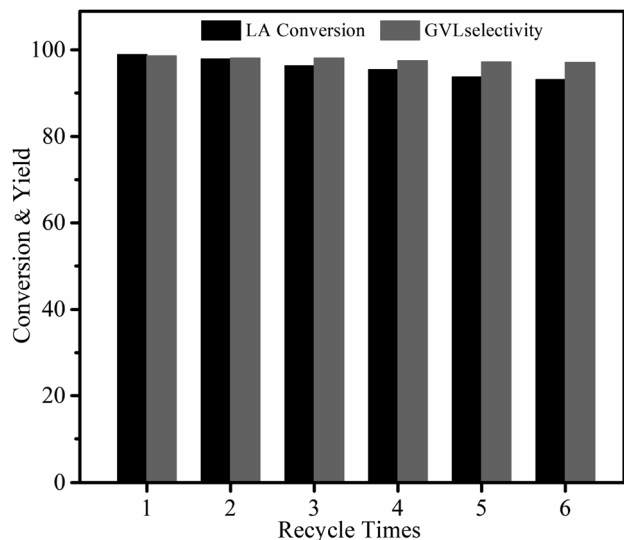


Fig. 8 Recyclability of Cu–Re(1 : 1)/TiO<sub>2</sub> catalyst for hydrogenation of LA to GVL. Reaction conditions: 0.5 g LA, 50 mg catalyst, 10 mL 1,4-dioxane, 4.0 MPa H<sub>2</sub>, 180 °C, 3 h, and 1000 rpm.

Re(1 : 1)/TiO<sub>2</sub> still kept high activity and selectivity, achieving a GVL yield of 90.3%. Analysis of the reaction solution after the sixth run revealed no detectable leach of Cu and Re, which confirmed the high stability of the catalyst in 1,4-dioxane. The comparison with other Cu-containing catalysts (Table S1†) indicated that Cu–Re(1 : 1)/TiO<sub>2</sub> developed in this work is a good catalyst for LA hydrogenation.

## 4. Conclusions

Hydrogenation of levulinic acid (LA) to  $\gamma$ -valerolactone (GVL) is one of the most promising reactions in the fields of biomass conversion into high value-added chemicals and biofuels. Cu-based catalysts are active non-noble catalysts for the hydrogenation of LA to GVL. However, hydrogenation of LA over monometallic Cu catalysts generally needs to be carried out at harsh reaction conditions due to the low activity of the catalysts. To obtain an efficient Cu-based catalyst, a series of Cu–Re/TiO<sub>2</sub> bimetallic catalysts prepared by an incipient wetness impregnation method were tested for the liquid phase hydrogenation of LA. The introduction of a suitable amount of Re into Cu/TiO<sub>2</sub> was demonstrated to remarkably improve the catalytic performance for the hydrogenation of LA to GVL. The Cu–Re/TiO<sub>2</sub> catalyst with a 1 : 1 molar ratio of Cu to Re achieved as high as 100% yield of GVL at 180 °C and 4.0 MPa H<sub>2</sub> for 4 h. The catalyst could be reused at least 6 times with slight activity loss. TEM results showed that the addition of Re decreased the average size of the metal nanoparticles, improved the dispersion of Cu, and formed Cu–Re alloy. H<sub>2</sub>-TPR results showed that the presence of Re promoted the reduction of Cu and there is a strong interaction between Cu and Re. XPS results evidenced the co-presence of the metallic Re and ReO<sub>x</sub>, and revealed that the addition of Re inhibited the oxidation of metallic Cu. The co-presence of Cu–Re bimetal and ReO<sub>x</sub> species in the samples,

and the improved Cu reducibility and dispersion were predominantly responsible for the good catalytic performance of Cu–Re/TiO<sub>2</sub> catalysts.

## Conflicts of interest

There are no conflicts to declare.

## Acknowledgements

This research was supported by the National Natural Science Foundation of China (21476211 and 21878269) and the Zhejiang Provincial Natural Science Foundation of China (LY18B060016).

## References

- 1 P. Gallezot, Conversion of biomass to selected chemical products, *Chem. Soc. Rev.*, 2012, **41**(4), 1538–1558.
- 2 L. T. Mika, E. Cséfalvay and Á. Németh, Catalytic conversion of carbohydrates to initial platform chemicals: chemistry and sustainability, *Chem. Rev.*, 2018, **118**(2), 505–613.
- 3 M. Besson, P. Gallezot and C. Pinel, Conversion of biomass into chemicals over metal catalysts, *Chem. Rev.*, 2014, **114**(3), 1827–1870.
- 4 D. M. Alonso, S. G. Wettstein and J. A. Dumesic, Gamma-valerolactone, a sustainable platform molecule derived from lignocellulosic biomass, *Green Chem.*, 2013, **15**(3), 584–595.
- 5 A. B. Jain and P. D. Vaidya, Kinetics of hydrogenation of furfuryl alcohol and  $\gamma$ -valerolactone over Ru/C catalyst, *Energy Fuels*, 2020, **34**(8), 9963–9970.
- 6 Y. Zhao, Y. Fu and Q. X. Guo, Production of aromatic hydrocarbons through catalytic pyrolysis of  $\gamma$ -valerolactone from biomass, *Bioresour. Technol.*, 2012, **114**, 740–744.
- 7 G. H. Wang, X. Q. Liu, B. Yang, C. L. Si, A. M. Parvez, J. Jang and Y. H. Ni, Using green  $\gamma$ -valerolactone/water solvent to decrease lignin heterogeneity by gradient precipitation, *ACS Sustainable Chem. Eng.*, 2019, **7**(11), 10112–10120.
- 8 U. Omoruyi, S. Page, J. Hallett and P. W. Miller, Homogeneous catalyzed reactions of levulinic acid: To  $\gamma$ -valerolactone and beyond, *ChemSusChem*, 2016, **9**(16), 2037–2047.
- 9 Z. H. Yu, X. B. Lu, C. Liu, Y. W. Han and N. Ji, Synthesis of  $\gamma$ -valerolactone from different biomass-derived feedstocks: Recent advances on reaction mechanisms and catalytic systems, *Renewable Sustainable Energy Rev.*, 2019, **112**, 140–157.
- 10 R. G. Weng, Z. H. Yu, J. Xiong and X. B. Lu, Effects of water in the heterogeneous catalytic valorization of levulinic acid into  $\gamma$ -valerolactone and its derivatives, *Green Chem.*, 2020, **22**(10), 3013–3027.
- 11 S. G. Wettstein, J. Q. Bond, D. M. Alonso, H. N. Pham, A. K. Datye and J. A. Dumesic, RuSn bimetallic catalysts for selective hydrogenation of levulinic acid to  $\gamma$ -valerolactone, *Appl. Catal., B*, 2012, **117–118**, 321–329.

- 12 L. E. Manzer, Catalytic synthesis of  $\alpha$ -methylene- $\gamma$ -valerolactone: a biomass-derived acrylic monomer, *Appl. Catal., A*, 2004, **272**(1–2), 249–256.
- 13 J. Feng, M. Li, Y. H. Zhong, Y. L. Xu, X. J. Meng, Z. W. Zhao and C. G. Feng, Hydrogenation of levulinic acid to  $\gamma$ -valerolactone over Pd@UiO-66-NH<sub>2</sub> with high metal dispersion and excellent reusability, *Microporous Mesoporous Mater.*, 2020, **294**, 109858.
- 14 M. Nemanashi, J. H. Noh and R. Meijboom, Hydrogenation of biomass-derived levulinic acid to  $\gamma$ -valerolactone catalyzed by mesoporous supported dendrimer-derived Ru and Pt catalysts: An alternative method for the production of renewable biofuels, *Appl. Catal., A*, 2018, **550**, 77–89.
- 15 S. H. Zhu, Y. F. Xue, J. Guo, Y. L. Cen, J. G. Wang and W. B. Fan, Integrated conversion of hemicellulose and furfural into  $\gamma$ -valerolactone over Au/ZrO<sub>2</sub> catalyst combined with ZSM-5, *ACS Catal.*, 2016, **6**(3), 2035–2042.
- 16 J. R. Wang, Y. Y. Wang, X. L. Tong, Y. W. Wang, G. Q. Jin and X. Y. Guo, Highly active Ir/SiC catalyst for aqueous hydrogenation of levulinic acid to  $\gamma$ -valerolactone, *Catal. Commun.*, 2020, **139**, 105971.
- 17 O. A. Abdelrahman, A. Heyden and J. Q. Bond, Analysis of kinetics and reaction pathways in the aqueous-phase hydrogenation of levulinic acid to form  $\gamma$ -valerolactone over Ru/C, *ACS Catal.*, 2014, **4**(4), 1171–1181.
- 18 J. J. Tan, J. L. Cui, G. Q. Ding, T. S. Deng, Y. L. Zhu and Y. W. Li, Efficient aqueous hydrogenation of levulinic acid to  $\gamma$ -valerolactone over a highly active and stable ruthenium catalyst, *Catal. Sci. Technol.*, 2016, **6**(5), 1469–1475.
- 19 O. Mamun, M. Saleheen, J. Q. Bond and A. Heyden, Investigation of solvent effects in the hydrodeoxygenation of levulinic acid to  $\gamma$ -valerolactone over Ru catalysts, *J. Catal.*, 2019, **379**(C), 164–179.
- 20 X. Q. Gao, S. H. Zhu, M. Dong, J. G. Wang and W. B. Fan, Ru nanoparticles deposited on ultrathin TiO<sub>2</sub> nanosheets as highly active catalyst for levulinic acid hydrogenation to  $\gamma$ -valerolactone, *Appl. Catal., B*, 2019, **259**, 118076.
- 21 A. Hommes, A. J. ter Horst, M. Koeslag, H. J. Heeres and J. Yue, Experimental and modeling studies on the Ru/C catalyzed levulinic acid hydrogenation to  $\gamma$ -valerolactone in packed bed microreactors, *Chem. Eng. J.*, 2020, **399**, 125750.
- 22 Z. J. Wei, J. T. Lou, C. M. Su, D. C. Guo, Y. X. Liu and S. G. Deng, An efficient and reusable embedded Ru catalyst for the hydrogenolysis of levulinic acid to  $\gamma$ -valerolactone, *ChemSusChem*, 2017, **10**(8), 1720–1732.
- 23 S. Dutta, I. K. M. Yu, D. C. W. Tsang, Y. H. Ng, Y. S. Ok, J. Sherwood and J. H. Clark, Green synthesis of gamma-valerolactone (GVL) through hydrogenation of biomass-derived levulinic acid using non-noble metal catalysts: A critical review, *Chem. Eng. J.*, 2019, **372**, 992–1006.
- 24 Z. He, H. Q. Lin, P. He and Y. Z. Yuan, Effect of boric oxide doping on the stability and activity of a Cu-SiO<sub>2</sub> catalyst for vapor-phase hydrogenation of dimethyl oxalate to ethylene glycol, *J. Catal.*, 2011, **277**(1), 54–63.
- 25 J. L. Gong, H. R. Yue, Y. J. Zhao, S. Zhao, L. Zhao, J. Lv, S. P. Wang and X. B. Ma, Synthesis of ethanol *via* syngas on Cu/SiO<sub>2</sub> Catalysts with Balanced Cu<sup>0</sup>-Cu<sup>+</sup> Sites, *J. Am. Chem. Soc.*, 2012, **134**(34), 13922–13925.
- 26 I. Orlowski, M. Douthwaite, S. Iqbal, J. S. Hayward, T. E. Davies, J. K. Bartley, P. J. Miedziak, J. Hirayama, D. J. Morgan, D. J. Willock and G. J. Hutchings, The hydrogenation of levulinic acid to  $\gamma$ -valerolactone over Cu-ZrO<sub>2</sub> catalysts prepared by a pH-gradient methodology, *J. Energy Chem.*, 2019, **36**, 15–24.
- 27 Q. Xu, X. L. Li, T. Pan, C. G. Yu, J. Deng, Q. X. Guo and Y. Fu, Supported copper catalysts for highly efficient hydrogenation of biomass-derived levulinic acid and  $\gamma$ -valerolactone, *Green Chem.*, 2016, **18**(5), 1287–1294.
- 28 T. G. Kelly and J. G. Chen, Metal overlayer on metal carbide substrate: unique bimetallic properties for catalysis and electrocatalysis, *Chem. Soc. Rev.*, 2012, **41**(24), 8021–8034.
- 29 W. T. Yu, M. D. Porosoff and J. G. G. Chen, Review of Pt-based bimetallic catalysis: from model surfaces to supported catalysts, *Chem. Rev.*, 2012, **112**(11), 5780–5817.
- 30 L. Zhang, J. B. Mao, S. M. Li, J. M. Yin, X. D. Sun, X. W. Guo, C. S. Song and J. X. Zhou, Hydrogenation of levulinic acid into gamma-valerolactone over *in situ* reduced CuAg bimetallic catalyst: Strategy and mechanism of preventing Cu leaching, *Appl. Catal., B*, 2018, **232**, 1–10.
- 31 B. Cai, X. C. Zhou, Y. C. Miao, J. Y. Luo, H. Pan and Y. B. Huang, Enhanced catalytic transfer hydrogenation of ethyl levulinate to  $\gamma$ -valerolactone over a robust Cu-Ni bimetallic catalyst, *ACS Sustainable Chem. Eng.*, 2017, **5**(2), 1322–1331.
- 32 D. Yanase, R. Yoshida, S. Kanazawa, Y. Yamada and S. Sato, Efficient formation of  $\gamma$ -valerolactone in the vapor-phase hydrogenation of levulinic acid over Cu-Co/alumina catalyst, *Catal. Commun.*, 2020, **139**, 105967.
- 33 Y. Takeda, Y. Nakagawa and K. Tomishige, Selective hydrogenation of higher saturated carboxylic acids to alcohols using a ReO<sub>x</sub>-Pd/SiO<sub>2</sub> catalyst, *Catal. Sci. Technol.*, 2012, **2**(11), 2221–2223.
- 34 M. D. Detwiler, P. Majumdar, X. K. Gu, W. N. Delgass, F. H. Ribeiro, J. Greeley and D. Y. Zemlyano, Characterization and theory of Re films on Pt(111) grown by UHV-CVD, *Surf. Sci.*, 2015, **640**, 2–9.
- 35 M. Tamura, K. Tokonami, Y. Nakagawa and K. Tomishige, Selective hydrogenation of crotonaldehyde to crotyl alcohol over metal oxide modified Ir catalysts and mechanistic insight, *ACS Catal.*, 2016, **6**(6), 3600–3609.
- 36 J. M. Keels, X. Chen, S. Karakalos, C. H. Liang, J. R. Monnier and J. R. Regalbuto, Aqueous-phase hydrogenation of succinic acid using bimetallic Ir-Re/C catalysts prepared by strong electrostatic adsorption, *ACS Catal.*, 2018, **8**(7), 6486–6494.
- 37 F. F. Yang, D. Liu, H. Wang, X. Liu, J. Y. Han, Q. F. Ge and X. L. Zhu, Geometric and electronic effects of bimetallic Ni-Re catalysts for selective deoxygenation of *m*-cresol to toluene, *J. Catal.*, 2017, **349**, 84–97.
- 38 Z. J. Wei, X. M. Zhu, X. S. Liu, H. Q. Xu, X. H. Li, Y. X. Hou and Y. X. Liu, Pt-Re/rGO bimetallic catalyst for highly selective hydrogenation of cinnamaldehyde to cinnamylalcohol, *Chin. J. Chem. Eng.*, 2019, **27**(2), 369–378.



- 39 X. M. Huang, K. T. Liu, W. L. Vrijburg, X. H. Ouyang, A. I. Dugulan, Y. X. Liu, M. W. G. M. T. Verhoeven, N. A. Kosinov, E. A. Pidko and E. J. M. Hensen, Hydrogenation of levulinic acid to  $\gamma$ -valerolactone over Fe-Re/TiO<sub>2</sub> catalysts, *Appl. Catal., B*, 2020, **278**, 119314.
- 40 K. Sing, D. Everett, R. Haul, L. Moscou, R. Pierotti, J. Rouquerol and T. Siemieniowski, Reporting physisorption data for gas/solid systems with special reference to the determination of surface area and porosity, *Pure Appl. Chem.*, 1985, **57**(4), 603–619.
- 41 V. G. Deshmane, S. L. Owen, R. Y. Abrokwhah and D. Kuila, Mesoporous nanocrystalline TiO<sub>2</sub> supported metal (Cu, Co, Ni, Pd, Zn, and Sn) catalysts: Effect of metal-support interactions on steam reforming of methanol, *J. Mol. Catal. A: Chem.*, 2015, **408**, 202–213.
- 42 X. Y. Jiang, G. H. Ding, L. P. Lou, Y. X. Chen and X. M. Zheng, Catalytic activities of CuO/TiO<sub>2</sub> and CuO-ZrO<sub>2</sub>/TiO<sub>2</sub> in NO + CO reaction, *J. Mol. Catal. A: Chem.*, 2004, **218**(2), 187–195.
- 43 B. Tapin, F. Epron, C. Especel, B. K. Ly, C. Pinel and M. Besson, Influence of the Re introduction method onto Pd/TiO<sub>2</sub> catalysts for the selective hydrogenation of succinic acid in aqueous-phase, *Catal. Today*, 2014, **235**, 127–133.
- 44 K. H. Kang, U. G. Hong, Y. Bang, J. H. Choi, J. K. Kim, J. K. Lee, S. J. Han and I. K. Song, Hydrogenation of succinic acid to 1,4-butanediol over Re-Ru bimetallic catalysts supported on mesoporous carbon, *Appl. Catal., A*, 2015, **490**, 153–162.
- 45 R. A. Rather, S. Singh and B. Pal, A Cu<sup>+</sup>/Cu<sup>0</sup>-TiO<sub>2</sub> mesoporous nanocomposite exhibits improved H<sub>2</sub> production from H<sub>2</sub>O under direct solar irradiation, *J. Catal.*, 2017, **346**, 1–9.
- 46 Z. F. Shao, C. Li, X. Di, Z. H. Xiao and C. H. Liang, Aqueous-phase hydrogenation of succinic acid to  $\gamma$ -butyrolactone and tetrahydrofuran over Pd/C, Re/C and Pd-Re/C catalysts, *Ind. Eng. Chem. Res.*, 2014, **53**(23), 9638–9645.
- 47 R. J. Shi, F. Wang, Tana, Y. Li, X. M. Huang and W. J. Shen, A highly efficient Cu/La<sub>2</sub>O<sub>3</sub> catalyst for transfer dehydrogenation of primary aliphatic alcohols, *Green Chem.*, 2010, **12**(1), 108–113.
- 48 A. Suknev, V. Zaikovskii, V. Kaichev, E. Paukshtis, E. Sadovskaya and B. Bal'zhinimaev, The nature of active sites in Pt-ReO<sub>x</sub>/TiO<sub>2</sub> catalysts for selective hydrogenation of carboxylic acids to alcohols, *J. Energy Chem.*, 2015, **24**(5), 646–654.
- 49 E. Hong, S. Bang, J. H. Cho, K. D. Jung and C. H. Shin, Reductive amination of isopropanol to monoisopropylamine over Ni-Fe/ $\gamma$ -Al<sub>2</sub>O<sub>3</sub> catalysts: Synergetic effect of Ni-Fe alloy formation, *Appl. Catal., A*, 2017, **542**, 146–153.